RESEARCH ARTICLE

Macromolecular Bioscience
www.mbs-journal.de

Development of a Tri-Layered Vascular Construct and In Vitro Evaluation of Endothelization

*Gozde E. Kole, Vasif Hasirci, and Deniz Yucel**

Advances in the development of vascular substitutes for small-sized arteries are ongoing because the present grafts do not entirely meet the requirements of native equivalents and are suboptimal in clinical performance. This study aims to develop a tri-layered vascular construct mimicking natural tissue using polyester blends and to investigate its endothelization through in vitro studies as a potential small-caliber vascular graft. The innermost layer is obtained by dip coating as a tubular porous film with a lumen diameter of 3 mm and a pore size of ≤8 µm. Circumferentially aligned electrospun fiber (diameter 100–800 nm) with a deviation angle of 15° are deposited over the porous film forming the intermediate layer. The random electrospun fibers (diameter 100–1100 nm) deviating at different angles are wrapped as the outermost layer. The mechanical properties of the tri-layered vascular construct are determined to be 44.80 ± 14.80 MPa for Young's modulus and 4.25 ± 0.75 MPa for ultimate tensile strength. MTS and cell behavior studies show that the isolated human umbilical cord vein endothelial cells proliferate and line the lumen of the vascular substitute. The vascular construct developed, with its biomimetic architecture, mechanical features, size, and endothelization, can be tested with in vivo studies.

1. Introduction

Cardiovascular diseases (CVDs), one of the leading causes of death worldwide, constitute a group of diseases that affect the heart and/or the blood vessels. There are various blood vessels that differ in type, size, and location. Vascular diseases are commonly seen in small- to medium-sized arteries, such as coronary, peripheral, and carotid arteries.[1] According to heart disease and stroke statistics, coronary heart disease, or coronary artery disease, is the most prevalent vascular disease and accounts for 41.2% of all CVD deaths.[2] The underlying cause of most vascular diseases is arteriosclerosis, narrowing of blood vessels due to plaque deposition on the vessel wall.[3] When blood flow is completely prevented due to occlusion, the obstructed site needs to be bypassed by surgery. Autologous grafts or artificial vascular grafts are used in these bypass operations.[4] The saphenous vein is the most widely used autograft in small-caliber arterial bypass surgeries because it is easy to access and harvest.[5] However, it may cause intimal hyperplasia, atherosclerosis, and/or aneurysm since the mechanical properties of the saphenous vein do not match those of the arteries that withstand high pressure.[6] In addition, the use of autografts has other drawbacks, such as limited availability, donor site morbidity, and the need for a second surgery.

Artificial vascular grafts are an alternative treatment approach to overcome the limitations of autografts. These vascular constructs can be implanted as tubular biomaterials or used as

G. E. Kole, D. Yucel
Graduate School of Health Sciences
Department of Medical Biotechnology
Acıbadem Mehmet Ali Aydınlar University (ACU)
Istanbul 34752, Turkey
E-mail: deniz.yucel@acibadem.edu.tr

G. E. Kole, V. Hasirci, D. Yucel
ACU Biomaterials A&R Center
Acıbadem Mehmet Ali Aydınlar University (ACU)
Istanbul 34752, Turkey

V. Hasirci
Faculty of Engineering and Natural Sciences
Department of Biomedical Engineering
Acıbadem Mehmet Ali Aydınlar University (ACU)
Istanbul 34752, Turkey

V. Hasirci, D. Yucel
Graduate School of Natural and Applied Sciences
Department of Biomaterials
Acıbadem Mehmet Ali Aydınlar University (ACU)
Istanbul 34752, Turkey

V. Hasirci
Middle East Technical University
BIOMATEN Center of Excellence in Biomaterials and Tissue Engineering
Ankara 06800, Turkey

D. Yucel
School of Medicine, Department of Histology and Embryology
Acıbadem Mehmet Ali Aydınlar University (ACU)
Istanbul 34752, Turkey

The ORCID identification number(s) for the author(s) of this article can be found under https://doi.org/10.1002/mabi.202300369

DOI: 10.1002/mabi.202300369

scaffolds in tissue engineering that are combined with vascular tissue cells. Vascular constructs made up of synthetic polymers such as polyethylene terephthalate (Dacron) and polytetrafluoroethylene (Teflon) meet the expectations of large-diameter (>6 mm internal diameter) blood vessels where the velocity of blood flow is high.[6,7] However, the clinical performance of small-diameter arterial substitutes (<5 mm internal diameter) with these materials is considered suboptimal.[6,8] The decrease in blood flow velocity in small-diameter arteries leading to thrombosis and hyperplasia after implantation results in low patency of vascular grafts.[7,9] There is a need for vascular graft biomaterials that can mimic the structural and functional properties of the natural blood vessels as much as possible. The ideal vascular construct, besides being biocompatible and not triggering an immune response, should not lead to thrombosis or blood coagulation; in other words, it should be hemocompatible and also allow endothelization.[6,10] Another important criterion is its mechanical properties. The vascular construct should have appropriate elasticity to withstand physical forces. The prominent challenge is to develop vascular constructs with biomimetic architecture; in that respect, the histological properties of the native tissue should also be taken into consideration in the design of the vascular construct. In general, the wall of a blood vessel consists of three concentric layers: tunica intima, tunica media, and tunica adventitia.[11] The innermost layer, tunica intima, is composed of a continuous monolayer of endothelial cells and subendothelial connective tissue. The intermediate layer, tunica media, is comprised of circumferentially arranged smooth muscle cells (SMCs). The outermost layer, tunica adventitia, mainly consists of irregular connective tissue. Thus, the scope of this study was to mimic this organization using biomaterials and produce a small-caliber, tri-layered vascular construct.

There are various polymers and different manufacturing options to develop a vascular graft with an appropriate porosity for nutrition and gas exchange, a desired topography for cell orientation, and suitable mechanical properties. Dip coating is a simple and effective technique for thin film production in tubular form to serve as a vascular construct.[12] By integrating a porogen and then leaching it out, porous films or foams with controllable pore sizes and interconnected pore structures could be formed.[13,14] The other fabrication method, electrospinning, is a versatile technique to obtain a three dimensional (3D) extracellular matrix (ECM)-like fibrous mesh structure with the desired topographical cues.[15,16] In the development of a vascular substitute, incorporation of the circumferentially aligned fibrous structure into the design of the vascular construct is a promising approach to achieve the analogous functions of native ECM and to enhance regeneration by promoting native tissue-like cell organization.[16,17] The Food and Drug Administration-approved synthetic polymers such as poly(ϵ-caprolactone) (PCL) and poly(D, L-lactide-co-glycolide) (PLGA) are among the polyesters that are widely utilized in artificial vascular grafts and are suitable for use in clinics.[8–21] PCL is appropriate for vascular constructs due to its biocompatibility, slow biodegradability, and elastic properties. Poly(L-lactide-co-D,L-lactide) (P(L-D, L)LA) is rigid and has controllable degradation and a high elastic modulus that will increase the mechanical strength. PLGA is highly biocompatible and its incorporation can make its blends quite extensible.[15] The mechanical properties of the vascular constructs can be tuned by using different polymers in varied ratios.

Earlier vascular studies had prioritized developing tubular substitutes without considering the nature of ECM.[22–24] Later studies focused on the development of various bi- or tri-layered vascular substitutes that take into account the architecture of native tissue.[18–20,25–33] A bi-layered biomimetic scaffold composed of aligned PCL electrospun fibers was produced to co-culture SMCs and endothelial cells.[29] In a study by Yuan et al. (2022), an electrospun mesh was combined with wet-spun fibers and smooth ink-jet printed film to form a tri-layered vascular graft consisting of poly(L-lactide-co-ϵ-caprolactone).[32] In another study, Huang et al. (2018) produced a tri-layered vascular graft by electrospinning and E-jet 3D printing of PCL through a biomimetic approach.[33] Even though the developed vascular constructs are promising, there is still a need to improve the mechanical and structural properties of the vascular substitutes, as well as their porosity and wall thickness, with the appropriate polymer composition and fabrication techniques. Consequently, the production of a small-caliber, tri-layered vascular graft that mimics the native vessel wall in its mechanical, functional, and topographical features is still a challenge.

The aim of this study was to develop a tri-layered vascular construct and evaluate its endothelization with in vitro studies. The vascular substitute was designed considering the histological features of the native artery by mimicking the intima, media, and adventitia layers of the blood vessel. The tri-layered vascular construct was prepared as follows: first, a tubular porous film was fabricated to serve as the innermost layer to house the endothelial cells, then circumferentially aligned electrospun fibers were deposited as the intermediate layer over the porous film, and lastly, a mesh of random electrospun fibers was wrapped around the aligned fibers as the outermost layer of the vascular construct. The morphology of the vascular construct and its layers were examined with a scanning electron microscope (SEM). The mechanical properties of the vascular construct after the formation of each layer were also studied. In addition, the wettability tests of the polymer blends used were conducted. The tri-layered vascular construct was evaluated in terms of its endothelization with in vitro studies using human umbilical vein-derived endothelial cells (HUVECs). After seeding HUVECs onto the lumen side of the construct, the cell number was determined at 7, 14, and 21 days of culture with the MTS assay. The endothelial cell (EC) behavior and the formation of the endothelium lining of the lumen were investigated by cytoskeleton and nuclei staining, as well as by immunostaining against endothelial cell markers.

2. Results and Discussion

2.1. Morphological Evaluation of the Tubular Porous Film

The inner layer of the tri-layered tubular construct was produced by dip coating followed by leaching of polyethylene glycol (PEG) to make it porous. The tubular porous film was to serve as the basal lamina for the adherence of the endothelial cells, similar to the tunica intima of the native blood vessel. The porosity and thickness of the film were optimized to provide the permeation of nutrients and waste while preventing cell penetration. To make this film porous, PEG (10%, w/v) was added to PCL-PLGA

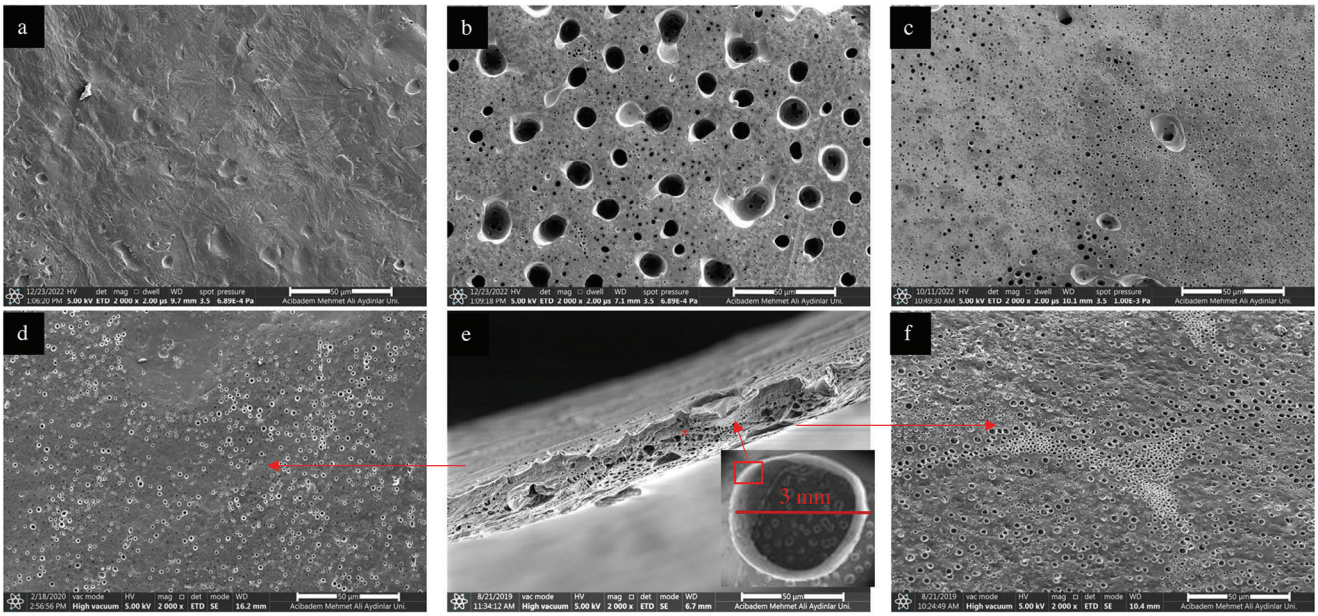

Figure 1. Scanning electron microscopy images of the tubular films prepared for the optimization of porosity and thickness. Films prepared by 15 dip coating using PCL–PLGA solution (10%, w/v; 8:2, w/w): a) without PEG (no pore) and b) with 10% PEG (porous). Porous films of PCL–PLGA (5%, w/v; 8:2, w/w) containing 10% PEG and dip coated c) ten times, and d–f) four times: d) inner surface, e) wall, and f) exterior surface. Inset of (e): cross-section view of the whole.

polymer solution (10%, w/v; 8:2, w/w) as porogen, and PEG was then leached out with distilled water. Almost no porous structures were observed on the tubular films prepared in the absence of PEG (**Figure 1**a), whereas those prepared with 10% PEG (w/v) displayed pores that were smaller than ca. 10 µm in diameter (Figure 1b,c). These results indicated that PEG was successfully removed from the tubular film leading to the formation of a porous film. However, the wall thickness of the obtained film was ca. 70 µm with heterogeneously sized pores (Figure 1b). To obtain a thinner film with more homogeneous pore size, the concentration of PCL–PLGA was decreased to half (5%), and the number of dip coatings cycles was reduced from 15 to 10. It was seen that the thickness of the tubular film was reduced from ca. 70 µm to ca. 46 µm; however, a few large pores were observed but with better homogeneity (Figure 1c). In the next step, the number of dip coating was decreased from ten to four while keeping the polymer concentration constant. Consequently, a thin tubular film with more homogeneous pores and a lumen diameter of 3 mm was successfully fabricated by dip coating four times using 5% PCL–PLGA (8:2; w/w) containing 10% PEG (Figure 1d–f). The wall thickness of the tubular porous film was 21.45 ± 1.07 µm (Figure 1e). The average porosity of the PCL–PLGA based film was calculated from three different SEM images using FIJI (ImageJ 1.53t). The porosity was 23.62 ± 1.25%, and homogeneous pore size was observed on both the internal and the external sides of the tube in the range of 1 to 5 µm and 4 to 8 µm, respectively (Figure 1d,f). The SEM images of the tube cross-section revealed porosity along the tube wall (Figure 1e, indicated with an asterisk). In other studies on vascular graft biomaterials, the thickness of the inner layers was in the range of 7–20 µm, which was close to the thickness determined in the present study.[32,34] However, these studies did not consider the porosity levels and pore size of the inner layer. The tubular film obtained in the present study may allow the passage of nutrients and wastes while preventing cell infiltration with a pore size that was less than the cell size [≤10 µm].[35] These results indicated that the inner porous tubular layer could support endothelial cell growth on the lumen side of the vascular construct.

2.2. Production and Morphological Analysis of the Circumferentially Aligned Electrospun Fibers

The intermediate layer of the tri-layered tubular construct was intended to consist of circumferentially aligned fibers obtained by electrospinning to mimic the tunica media of the native blood vessels, in which the SMCs are circumferentially aligned. During optimization, various electrospinning process parameters and polymer concentrations were tested to obtain uniform fibers without beads (data not provided). A uniform, bead-free fiber structure was produced using 5% PCL–P(L–D, L)LA–PLGA (4:4:2, w/w, dichloromethane:dimethlyformamide (DCM: DMF), 19:1, v/v) under 15 kV voltage, at 25 cm distance, 3000 rpm mandrel rotation speed, and with 5–20 µL min^{-1} flow rate (**Figure 2**). A tubular electrospun fibrous mat was successfully obtained using a metal rod in the mandrel system (Figure 2a). It was thought that the fiber alignment could be improved by altering the flow rate because the rotation speed of the system could not be increased >3000 rpm. Therefore, keeping the other parameters constant, different flow rates (at 5, 10, 15, and 20 µL min^{-1}) were used to obtain aligned fibers. It was observed that a reduction in the flow rate from 20 to 15 µL min^{-1} increased the alignment of the fibers (Figure 2c,d), and a further reduction to 10 and 5 µL min^{-1} led to the formation of less aligned fibers (Figure 2e,f). Similarly,

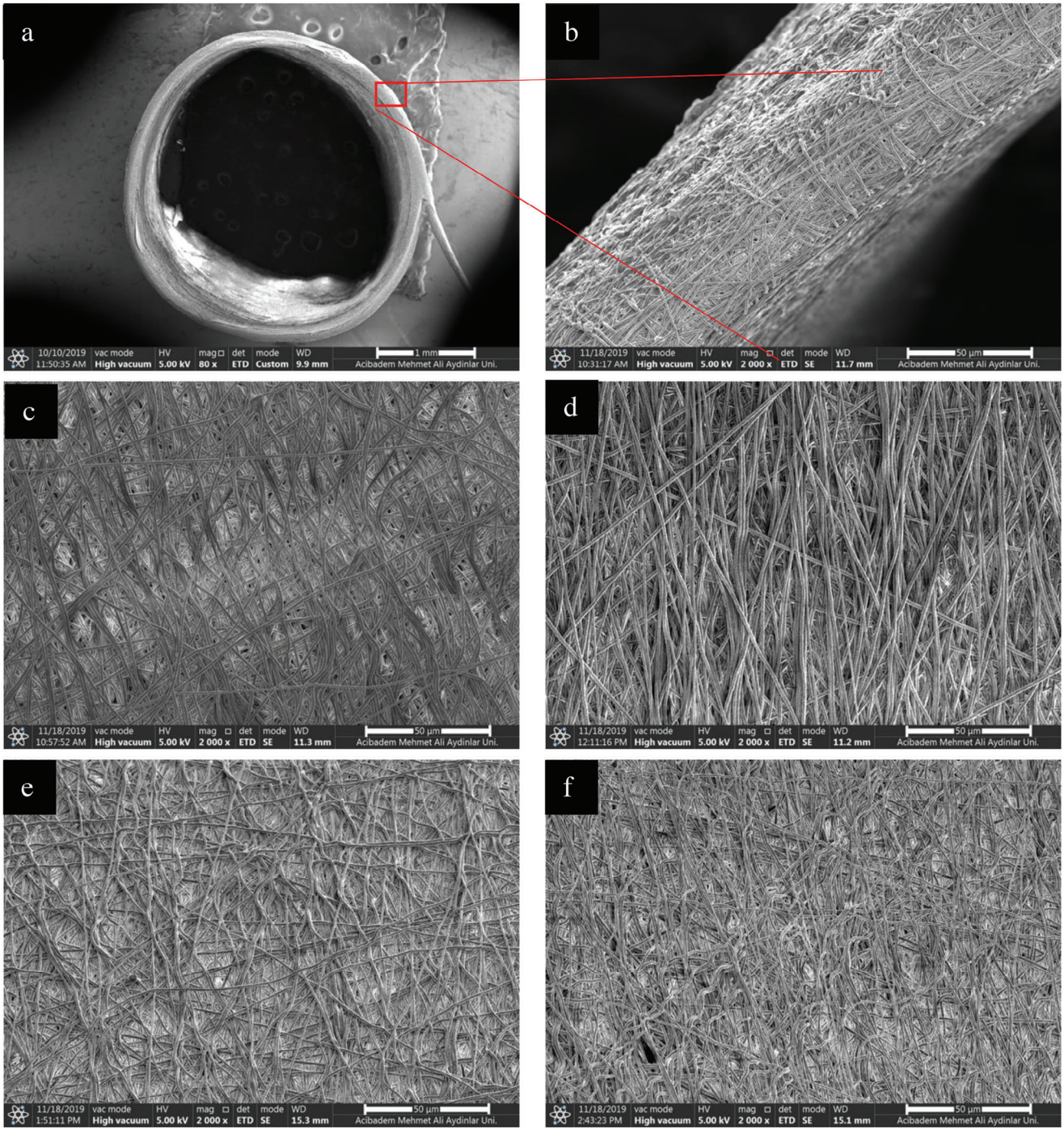

Figure 2. Scanning electron microscopy images of the electrospun mats prepared with PCL–P(L–D,L)LA–PLGA (5%, 4:4:2, w/w; in DCM:DMF, 19:1, v/v) under flow rates of a–c) 20, d) 15, e) 10, f) 5 µL min^{-1}.

Gou Y. et al. (2014) observed a decrease in fiber alignment below or above the optimum flow rate.[36] In the present case, it was concluded that the best fiber alignment was obtained at the flow rate of 15 µL min^{-1}. In addition to the rotation speed of the mandrel, the voltage and flow rate affect fiber alignment during the electrospinning process, and these parameters should be carefully balanced to achieve fiber alignment.[37,38] SEM revealed that uniform, bead-free, parallel fibers were produced using 5% polymer solution under the optimized conditions of 15 kV voltage, 15 µL min^{-1} flow rate, 25 cm distance, and 3000 rpm rotation speed of the mandrel system. The intermediate, circumferentially aligned fibrous layer of the tri-layered vascular construct obtained using these parameters was used in the rest of the studies.

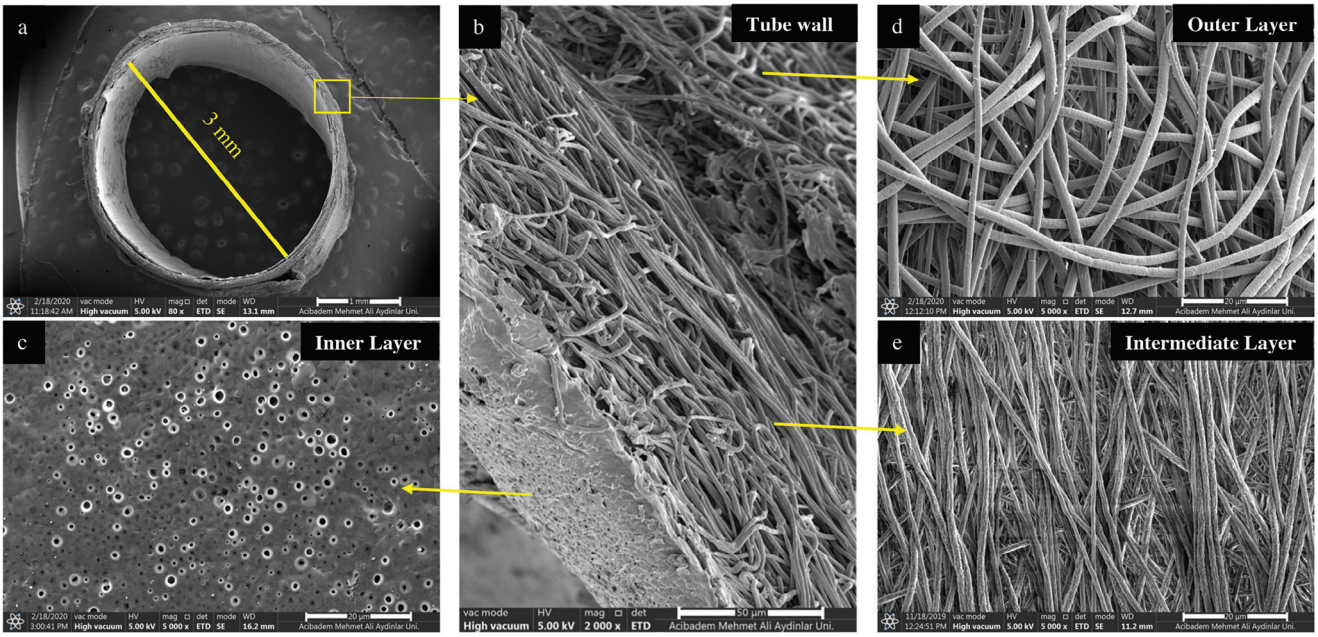

Figure 3. Scanning electron microscopy images of the tri-layered vascular construct. a) Cross-sectional view of the entire tubular construct and b) the tube wall. Micrographs of c) the inner porous film (PF) side, d) the outer random fibrous mat side, and e) the intermediate circumferentially aligned fibrous mat of the constract.

2.3. Assembling the Tri-Layered Vascular Construct by Integrating the Electrospun Fibers over the Tubular Porous Film

The tri-layered tubular construct was successfully obtained by producing each layer over the other in the following order: fabrication of the tubular porous film as the innermost layer, collection of the circumferentially aligned electrospun fibers over the porous film as the intermediate layer, and wrapping of the random electrospun fibers over the aligned fibers as the outermost layer (**Figure 3**). The tubular porous film produced by dip coating four times using 5% PCL-PLGA (8:2, w/w) containing 10% PEG solution had a thickness of 21.45 ± 1.07 µm (Figure 3c). The porous film displayed homogeneously distributed pores with pore sizes ranging from 1 to 8 µm. The circumferentially aligned mat was deposited over the tubular porous film using 5% PCL-P(L-D, L)LA-PLGA (4:4:2, w/w, DCM: DMF, 19:1, v/v) without any gap between the two layers. SEM images indicated that the thickness of the intermediate layer was 57.07 ± 4.39 µm, and the fibers were aligned perpendicular to the lumen diameter (Figure 3e). To imitate the tunica adventitia of the native blood vessels, the external layer of the construct was fabricated as a random fibrous mat by electrospinning using the same polymer solution under the same optimized parameters, except for the rotational speed of the mandrel system. Random topography was obtained at 500 rpm mandrel rotation speed (Figure 3d). The thickness of the outermost layer, the random fibrous mat, was 67.32 ± 0.89 µm.

The size and topography of the fibers affect the behavior of cells and make these scaffolds important considerations for tissue engineering approaches. Cells spread more on fibers in the nanometer range than on the micron scale.[39] The cells sense the topography of the oriented fibers and are aligned along the fiber direction, while they spread in all directions on random fibers.[40] The fiber diameter and deviation angle, indicating fiber orientation, were measured using the FibroQuant 1.3 image processing software (**Figure 4**). In the intermediate, circumferentially aligned fibrous mat layer, 90% of the fibers had diameters in the range of 100–800 nm, with more than half having fiber diameters of 200–400 nm (Figure 4a). The fiber orientation graph of the intermediate layer indicated that most of the fibers (ca. 55%) were aligned in a parallel manner with a ± 15° deviation angle (Figure 4b). The intermediate layer was designed as circumferentially aligned fibers to house and align the cells along the fibers for further tissue engineering and/or in vivo implantation studies. One of the studies reported that the cells had a spindle-like morphology and were spread along the fibers when cultured on the fibers aligned at ± 30 ° compared to the cells on random fibers.[40] Considering this information, the submicron-sized fibers aligned mostly at a ± 15° deviation angle would provide a suitable environment for cell attachment and alignment. Thus, as intended, the intermediate layer was comprised of circumferentially aligned fibers. SEM image analysis showed that the outermost layer of the construct was composed of fibers with a wide range of diameters (100–1100 nm) and that ca. 35% of the fibers were in the range of 800–1000 nm (Figure 4c). The fiber orientation graph of the outer layer showed that there was no particular fiber direction and most of the fibers deviated at different angles (Figure 4d). Although the same polymer solution was used in the electrospinning of the intermediate and outer layers, the difference in fiber diameter and orientation was due to the use of two different collectors that varied in diameter and rotation speed. It was reported that as the fiber diameter increased in the random electrospun mats, the average pore size of the mats increased proportionally with the fiber diameter.[39] As a result,

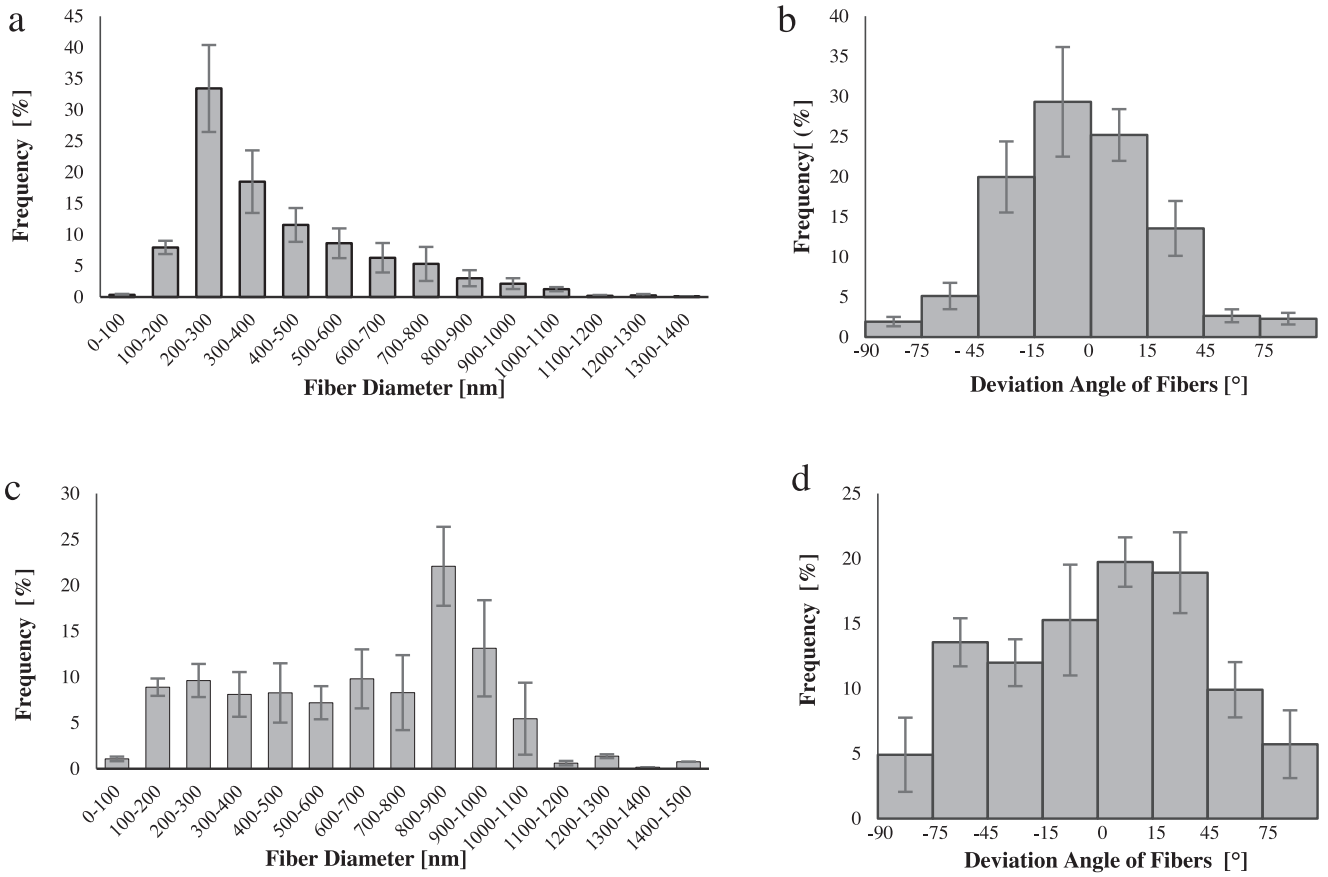

Figure 4. Distribution of diameters and deviation angles of the fibers. a,b) The circumferentially aligned fibrous mat as the intermediate layer and c,d) the random fibrous mat as the outer layer of the construct.

the random fibrous mat obtained could serve as a loose mesh to mimic the loose connective tissue of the tunica adventitia of the native blood vessel.

2.4. Mechanical Properties and Wettability Analysis of the Tri-Layered Vascular Construct

Blood vessels face an environment of mechanical stress, and therefore the mechanical properties of vascular substitute should mimic those of the native blood vessel as much as possible. In this study, Young's modulus of the vascular construct was calculated using the tensile stress–strain curve. It was determined that the Young's modulus of the inner porous film in the longitudinal direction was 30.00 ± 3.80 MPa. This value increased to 50.40 ± 9.60 MPa upon deposition of the circumferentially aligned fibers over the porous film, and this increase could be due to the presence of P(L-D, L)LA and the compact, aligned mesh form of the intermediate layer. The final tri-layered construct had a Young's modulus of 44.80 ± 14.80 MPa. A slight decrease in this value was observed after the integration of the random fibrous mesh. It was reported that random fibers had a lower mechanical tensile strength than aligned fibers [41] and this is expected. Thus, in the present study, the incorporation of the random fibrous mesh as the outermost layer increased the thickness of the test sample while it did not contribute as much to the mechanical properties as the aligned layer leading to the decrease of Young's modulus in the tri-layered vascular construct. The Young's modulus of the tri-layered vascular graft is similar to those of the biomaterial vascular grafts composed of PCL and its blends. For instance, it was reported that PCL/polyurethane based single layer vascular graft had a tensile strength of ≈60.48 ± 8.01 MPa.[42] The elasticity of the vascular graft developed can be enhanced by integrating natural polymers to match the mechanical properties of the saphenous vein (23.70 MPa), which is the most commonly used autograft in bypass surgery.[43] In one of the studies, it was revealed that blending PCL with natural polymers such as elastin and collagen improved the mechanical performance of the electrospun vascular grafts.[44] The ultimate tensile strength (UTS) values after the formation of each layer of the tri-layered vascular construct starting from the inner layer were 3.34 ± 0.76, 5.44 ± 0.72, and 4.25 ± 0.75 MPa, respectively, in the longitudinal direction. The UTS values of the saphenous vein and small-sized arteries such as the mammary artery were reported as 6.30 and 4.30 MPa, respectively, in the longitudinal direction.[43,45] In studies reported in the literature, determined the UTS values of the vascular grafts were to be 1.10, 11.47, and 0.36 MPa.[43,45,46] The ultimate strength of the tri-layered construct developed in this study was slightly lower than that of the saphenous vein and almost the same as that of the mammary artery.

The wettability of PCL–PLGA and PCL–P(L–D, L)LA–PLGA was studied with the contact angle measurements. The contact angles for the materials PCL–PLGA and PCL–P(L–D, L)LA–PLGA were $95.32 \pm 1.65^{\circ}$ and $124.51 \pm 1.67^{\circ}$, respectively. A contact angle between 90° and 180° is considered hydrophobic.[47] The vascular construct should provide the endothelization on its lumen side, and allow cell growth in its intermediate and outer layers such as, like SMCs of the tunica media and fibroblasts of the tunica adventitia. Therefore, surfaces with moderate levels of hydrophilicity (contact angle in the range of 40°–70°) would be more favorable for the attachment of HUVECs and other cells to the surfaces. It was thought that the surfaces could be made hydrophilic by a protein coating to facilitate cell attachment. Thus, gelatin was coated on the lumen side of the tri-layered vascular construct to enhance endothelization and allow cell growth on this surface in later studies. The contact angles of the 1% gelatin-coated PCL–PLGA and PCL–P(L–D, L)LA–PLGA surfaces were $40.28 \pm 2.08^{\circ}$ and $45.83 \pm 4.17^{\circ}$, respectively. These results indicated that the gelatin coating rendered the hydrophobic surfaces more hydrophilic, which could provide surfaces suitable for cell attachment.

2.5. Isolation and Characterization of Human Umbilical Vein Endothelial Cells

In this study, HUVECs were enzymatically isolated from the umbilical cord vein (**Figure 5**a). It was observed that HUVECs adhered to the surface of tissue culture polystyrene (TCPS) after one day of isolation, and were initially clustered (Figure 5b inside the circle). In addition, HUVECs exhibited a characteristic morphology of cobblestone appearance. The isolated cells proliferated in the EC growth medium, and reached 70–80% confluency after five days of culture (Figure 5c). Cells were characterized by confirming the expression of EC-specific markers such as CD31 and vWF with immunocytochemistry. The endothelial marker CD31 is a specialized cell adhesion molecule located in the intercellular contact regions. The other selected marker for endothelial cells, von Willebrand Factor (vWF), is a glycoprotein localized in Weibel-Palade bodies, which are endothelial-specific organelles, and play a crucial role in the maintenance of the non-thrombogenic barrier function of ECs. Immunocytochemistry results showed that the isolated cells expressed CD31 on their cell membranes along cell borders and vWF in their cytoplasm, as expected from ECs (Figure 5d,e). In conclusion, HUVECs were successfully isolated from the umbilical vein and cultured efficiently in the EC growth medium, while preserving their characteristic properties under in vitro conditions.

2.6. In Vitro Evaluation Of Endothelization of the Tri-Layered Vascular Construct

Blood vessels are lined with an epithelium called the endothelium composed of a single layer of elongated, polygonal ECs that exhibit characteristic cobblestone morphology. ECs are very crucial for native tissue because they maintain homeostasis, act as a non-thrombogenic membrane between the underlying tissue and blood to prevent thrombus formation, and regulate the immune response.[11] Therefore, in addition to biocompatibility and mechanical properties, providing endothelization is a crucial criterion for the performance of vascular constructs or scaffolds in the fields of biomaterials and tissue engineering. In addition, the ECs lining of the lumen of the vascular construct could offer a solution to prevent intimal hyperplasia and thrombosis, which are challenges in small-caliber vascular substitutes.[6,48] Endothelization is also essential for neovascularization, which depends on the ECM secretion of the adhered ECs.[49] The endothelium, a monolayer of ECs, not only acts as a barrier for thrombus formation but also serves as the foundation for angiogenesis, enabling the formation of new blood vessels in response to tissue needs and repair processes. Therefore, promising vascular substitutes should be composed of appropriate materials using suitable fabrication techniques that produce convenient topography, allowing adherence and spreading of ECs to achieve endothelization.[50,51]

In the present study, the endothelization of the developed, tri-layered vascular construct was assessed under in vitro conditions by seeding HUVECs into the lumen side of the tubular construct. The viability and proliferation of these HUVECs on the lumen side were investigated using the MTS assay (**Figure 6**a). In addition, the morphology and organization of these cells on the luminal surface of the construct were studied using phalloidin-DAPI staining (Figure 6b–d). MTS assay indicated that HUVECs adhered to the lumen side of the construct and increased in number (Figure 6a). This increase in the number of HUVECs was statistically significant and the cell number was threefold higher on day 14 compared to the cell number on day 7 ($p < 0.01$) The growth of the HUVECs was continued on the 21st day of culture, despite an insignificant reduction in cell number ($p > 0.05$), which might be due to confluency of HUVECs. Morphology analysis of these HUVECs confirmed the MTS assay results (Figure 6). HUVECs adhered and spread on the luminal side of the construct over time, especially on the 14th day of culture (Figure 6b–d). As the cells further multiplied over time, they spread entirely throughout and thus lined the luminal surface of the inner layer of the vascular construct, as expected for endothelization (Figure 6c,d). Immunocytochemistry results showed that the HUVECs preserved the expression of specific endothelial cell markers, CD31, along the borders and vWF within the cytoplasm on the luminal surface of the vascular construct (**Figure 7**a,b). Immunostaining against CD31 and SEM results showed that HUVECs preserved their cobblestone morphology and formed a continuous endothelial lining on the luminal surface of the vascular construct (Figure 7d,e). All in vitro studies revealed that HUVECs were viable, proliferated, spread, and occupied the lumen of the vascular structure over time. They conserved their characteristic morphology and expression of proteins.

3. Conclusion

In this study, a small-caliber, tri-layered vascular construct was developed considering the layers of the native blood vessels. The vascular construct with a lumen size of 3 mm diameter was composed of three layers: a tubular porous film forming the innermost layer, the intermediate layer consisting of circumferentially aligned fibers, and the outermost layer formed by a random electrospun mesh. The tubular porous film was produced by dip coating to mimic the tunica intima of the native artery. The obtained

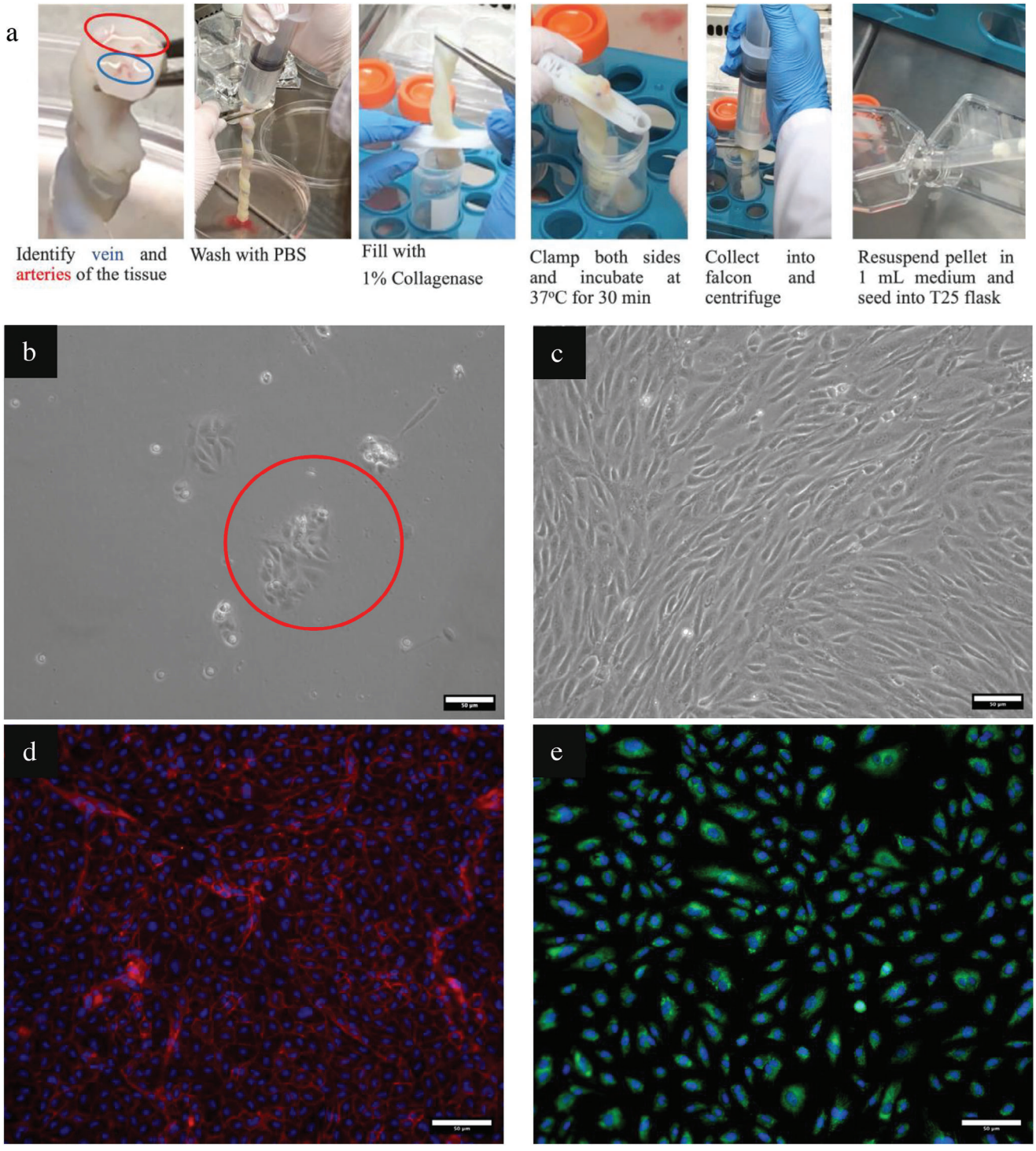

Figure 5. Isolation and culture of human umbilical vein endothelial cells (HUVECs). a) Enzymatic isolation of HUVECs from the umbilical cord vein. Light microscopy images of HUVECs on the gelatin-coated TCPS on days b) one and c) five (the cell cluster is encircled in red). Fluorescence micrographs of HUVECs after immunostaining for the expression of endothelial cell markers d) CD31(red) and e) vWF (green) and counterstaining nuclei with DAPI (blue).

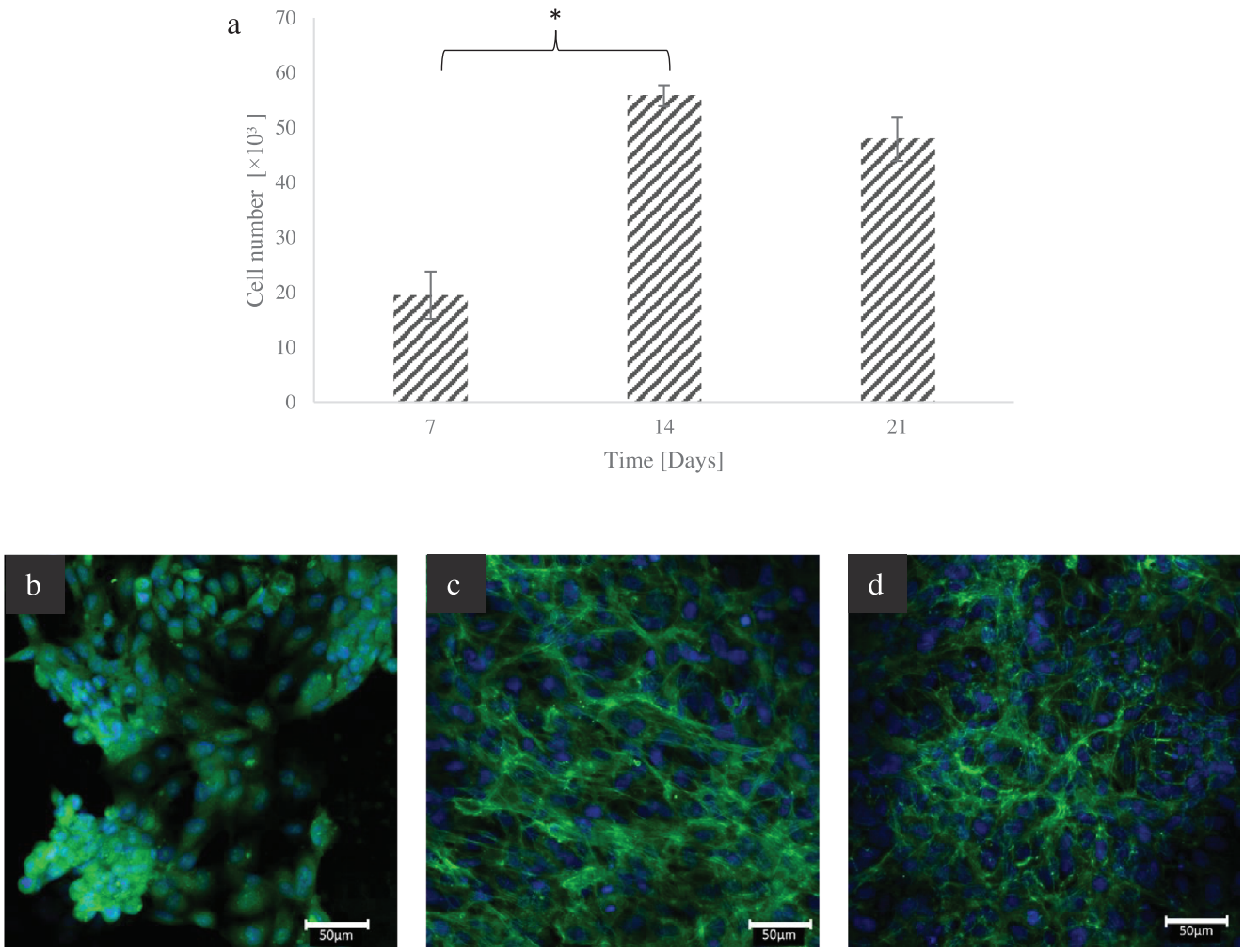

Figure 6. Growth of human umbilical cord vein endothelial cells (HUVECs) on the lumen side of the vascular construct. a) Proliferation of the HUVECs on the construct during three weeks of culture ($^{*}p < 0.01$). Confocal micrographs of HUVECs stained with FITC-phalloidin (green) and DAPI (blue) on Day b) 7,c) 14 and d) 21 of culture .Scale bars: 50 µm.

porosity (23.62 ± 1.25%) and pore size (≤ 8 µm) of the film were appropriate to allow the passage of medium and gas as well as to prevent cell penetration, as intended. Considering the tunica media of the native blood vessel, the intermediate layer of the vascular comprised circumferentially aligned fibers that were successfully deposited on the tubular porous film via electrospinning. A random electrospun fibrous mat was wrapped over the aligned fibers as the outermost layer to mimic the tunica adventitia. The construct had a lumen diameter of 3 mm, which is within the range of small–caliber vascular grafts. The tri-layered vascular construct exhibited encouraging mechanical properties and allowed endothelization.

Obtaining arterial substitutes with a diameter of <6 mm is still a challenge in biomaterials and tissue engineering. The vascular substitute developed could potentially address this issue. Consequently, the tri-layered vascular construct developed in the present study could be considered for use as a small–caliber vascular substitute with its biomimetic architecture, encouraging mechanical properties, and high endothelization potential without collapsed. In addition, the vascular construct coated with cell adhesion proteins could have the potential to be used for further in vivo studies. Thus, it would be a promising treatment approach for coronary artery disease to save millions of lives in the clinic.

4. Experimental Section

Materials: Poly(ϵ-caprolactone) (PCL, ca. Mw 124 000 g mol^{-1}), poly(D,L-lactide-co-glycolide) (PLGA, 50:50, ca. Mw 153 000 g mol^{-1}) and poly(L-lactide-co-D, L-lactide) (P(L-D, L)LA, 70:30, ca. Mw 1 500 000 g mol^{-1}) were purchased from PURAC, Corbion (Netherland). Polyethylene glycol (PEG, Mw 1000 Da) was purchased from Fluka, Biochemica (Switzerland). N, N-dimethylformamide (DMF) was obtained from Merck (USA). Hank's Balanced Salt Solution (HBSS) was purchased from Capricorn Scientific (Germany). An endothelial growth medium kit (EGM-2, C-22111) was obtained from PromoCell (Germany). Platelet Endothelial Cell Adhesion Molecule (PECAM-1, also known as CD31) was purchased from Aligent, Dako (USA). Rabbit anti-human vWF was purchased from Abcam (UK). Goat anti-rabbit Alexa Fluor 488 was purchased from Millipore (Germany). Goat anti-mouse Alexa Fluor 555 was purchased from ThermoFisher (USA). Phalloidin, DAPI, and bovine serum albumin (BSA) were purchased from Sigma (USA). MTS was purchased from Promega (USA).

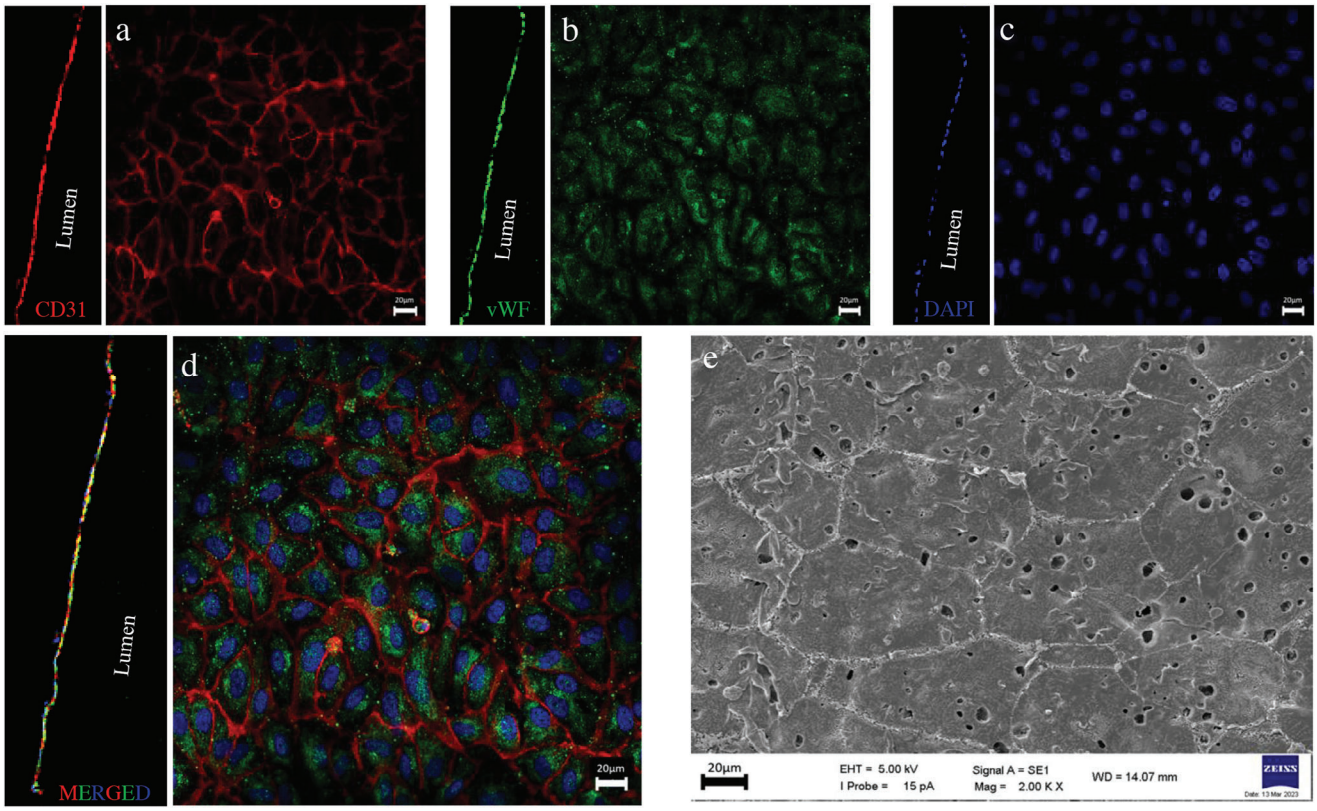

Figure 7. Laser scanning confocal and scanning electron microscopy images of human umbilical cord vein endothelial cells HUVECs on the lumen side of the vascular construct. The cells were immunostained against a) CD31 (red) and b) vWF (green) and also counterstained with c) DAPI (blue) for the nuclei. d) Merged image of CD31, vWF, and DAPI. Scale bars: 20 µm. e) Morphological analysis of HUVECs on the inner layer of the vascular construct with SEM.

Production of the Tri-Layered Vascular Construct: *Preparation of the tubular porous film*: The tubular porous film as to be the inner layer of the tri-layered construct was fabricated by dip coating using a blend of PCL-PLGA (5% or 10%, w/v, 8:2, w/w, in DCM). Stainless steel metal rods (316LVM Medical Grade, diameter 3 mm, length 13 cm) were dipped into PCL-PLGA solution, containing PEG (10%, w/v) as a porogen, and the solvent was air-dried at room temperature. Dip coating was repeated 4–15 times to obtain a structure with an appropriate thickness. Polymeric film-coated rods were placed in dH_2O to leach out PEG and obtain a tubular porous film. Samples were freeze-dried to preserve the porous structure.

Fabrication of the electrospun fibrous mats and establishment of the tri-layered vascular construct: The circumferentially aligned and random fibrous mats were produced by electrospinning using a rotating mandrel system to obtain the intermediate and outer layers of the vascular construct, respectively. A blend of PCL-P(L-D, L)LA-PLGA (5%, w/v, 4:4:2, w/w) prepared in DCM: DMF (19:1, v/v) was used in the fabrication of both the circumferentially aligned and the random fibers. The electrospinning process parameters of voltage (10–15 kV), distance between the needle and the collector (20–25 cm), flow rate of the polymer solution (5–20 µL min^{-1}), and rotation speed of the mandrel (500/3000 rpm) were optimized to obtain uniform, bead-free fibers and to achieve aligned and random fibers. Upon optimization studies, both aligned and random electrospun fibers were fabricated using the following conditions: a distance of 25 cm, a flow rate of 15 µL min^{-1}, and a voltage of 15 kV. The metal rod (length 13 cm, diameter 3 mm) coated with the thin, porous film prepared above was used as the collector in the mandrel system. The circumferentially aligned fibers as the intermediate layer of the tri-layered vascular construct were collected over the film using the determined parameters at a rotating speed of 3000 rpm. The random fibrous mat was collected under optimized conditions on an uncoated metallic rod (diameter 4 mm) at a rotation speed of 500 rpm. Then, the random fibrous mat was wrapped over the circumferentially aligned fibrous mat to form the outer layer of the tri-layered vascular construct.

Characterization of the Tri-Layered Vascular Construct: *Morphology analysis with Scanning Electron Microscopy*: The morphology and topography of the components of the tri-layered vascular construct, including the tubular porous film, circumferentially aligned fibrous mat, and random fibrous mat, were examined with SEM. All samples were coated with a 55 nm thick gold layer under vacuum by a sputter coater (Leica, EM ACE600), and the images were obtained with a SEM (Thermo, Quatrro ESEM) at 5 kV.

The fiber diameter distribution and orientation were analyzed with Fibro Quant 1.3 software using three SEM images obtained from different areas of the electrospun fibrous mat. The diameter and the deviation angles of fibers indicating their orientation were determined by taking a selected fiber as the reference. Histograms were plotted with the percentage of fibers with respect to their diameter and orientation.

Mechanical tests: The tensile mechanical properties of the construct were determined with a mechanical tester (Shimadzu, AGS-X Series Universal Test Machine) after each layer formation. Tests were performed with the inner layer porous film, the bi-layered structure including the porous film and the circumferentially aligned fibrous mat, and the tri-layered final construct. The tubular samples (length 2 cm) were cut longitudinally before testing. The sample length between the clamps was 10 mm, and the tensile test was done with 1 mm min^{-1} test speed ($n = 4$). The stress–strain graphs were obtained for each sample, and then Young's modulus and UTS values were determined from these plots.

Wettability analysis: The water wettability of the PCL-PLGA and PCL-P(L-D, L)LA-PLGA blends was determined with a goniometer (Krüss, DSA25).

The solutions of PCL-PLGA (5%, w/v, 8:2, w/w) and PCL-P(L-D, L)LA-PLGA (5%, w/v, 4:4:2, w/w) were poured onto glass slides, and the solvent was evaporated by air-drying to obtain non-porous films. Drops of distilled water were placed at five different points on the polymeric films, and the angles were measured using ADVANCE software. The contact angle θ was found according to Young's Equation (I):

$$\sigma_{sg} = \sigma_{sl} + \sigma_{lg} \times cos\theta \quad \text{(I)}$$

where the σ_{lg} is the surface tension of the liquid, σ_{sl} is the interfacial tension between the solid and the liquid, σ_{sg} the surface free energy of the solid.

In Vitro Evaluation of Endothelization of the Tri-Layered Vascular Construct: *Isolation and culture of human umbilical vein endothelial cells*: HUVECs were isolated and used with the approval of Acıbadem University and Acıbadem Healthcare Institutions Medical Research Ethics Committee (ATADEK, 2018-2/64). The umbilical cord was obtained from the donor after birth with the informed consent of the mother and was placed in HBSS containing penicillin/streptomycin (100 units mL^{-1}pre100 mg mL^{-1}). HUVECs were isolated from the human umbilical cord vein by the enzymatic method within 24 h. The vein lumen was washed with phosphate-buffered saline (PBS, 10 mM, pH 7.4), then filled with 0.1% collagenase solution (w/v, in PBS) and incubated at 37 °C for 30 min. The suspension was collected into 50 mL falcon tubes and centrifuged at 1500 rpm for 5 min. The cell pellet was resuspended in endothelial cell growth medium composed of EGM-2 containing Epidermal Growth Factor (EGF) (5 ng mL^{-1}), basic Fibroblast Growth Factor (bFGF) (10 ng mL^{-1}), Insulin-like Growth Factor (IGF) (20 ng mL^{-1}), Vascular Endothelial Growth Factor (VEGF) (0.5 ng mL^{-1}), ascorbic acid (1 µg mL^{-1}), heparin (22.5 µg mL^{-1}), hydrocortisone (0.2 µg mL^{-1}), fetal calf serum (FCS, 2%) and penicillin/streptomycin (100 units mL^{-1}per100 mg mL^{-1}). The cells were then cultured in gelatin (1%, w/v, in PBS) coated TCPS flasks at 37 °C in a humidified 5% CO_2 incubator, and the growth medium was refreshed every three days. When the cells reached ≈80% confluency, they were detached from the surface with 0.05% Trypsin-EDTA and subcultured, or cryopreserved in 10% dimethyl sulfoxide at liquid nitrogen vapor until further use.

Characterization of the isolated HUVECs: Identification of HUVECs was performed with immunocytochemistry by investigating the expression of endothelial-specific markers, CD31, and vWF. HUVECs were seeded on 1% gelatin-coated 24 well plate at a density of 5×10^3 cells/well and cultured in the growth medium at 37 °C in a humidified 5% CO_2 incubator. After three days of culture, the cells were fixed with 4% paraformaldehyde (PFA) for 30 min at room temperature (RT). After washing with PBS, the cells were incubated in 100 mM glycine for 15 min, and then washed with PBS three times. The cells were permeabilized with 0.1% Triton X-100 (in PBS) for 10 min at RT. After washing with PBS, the cells were incubated in a blocking solution (1% bovine serum albumin (BSA) in PBS) for 30 min at 37 °C. The cells were incubated overnight at + 4 °C with the primary antibodies, rabbit anti-human vWF (1:250), and mouse anti-human CD31 (1:40). The cells were then washed with PBS and incubated with the appropriate fluorescence-labeled secondary antibodies, goat anti-rabbit Alexa Fluor 488 (1:100) and goat anti-mouse Alexa Fluor 555 (1:200). The cells were washed with PBS and then counterstained with DAPI (1:5000) for 10 min at RT. The cells were rinsed with PBS and examined under a fluorescence microscope (Zeiss, Axiovert A1).

Endothelial cell behavior on the vascular construct: Cellular activity and morphology of HUVECs on the vascular construct were studied with the MTS assay and microscopically after phalloidin-DAPI staining, respectively. The tubular vascular constructs (lumen diameter 3 mm, length 1 cm) were sterilized with 70% EtOH for 2 h and dried overnight. The lumen side of the construct was coated with 1% gelatin (in PBS) for 2 h at 37 °C, and the vascular constructs were ready to be seeded with cells. HUVECs were detached from TCPS flasks and seeded onto the lumen side at a density of 2×10^4 cells/construct to study cell behavior on the vascular constructs (n = 3).

Cell numbers on the vascular constructs were determined with the MTS assay on days 7, 14, and 21 of the culture. The vascular constructs were transferred to new 24 well plates. The working solution of 10% MTS was prepared in an endothelial cell growth medium and added to the HUVEC seeded tubular constructs. The cells were incubated for 2 h at 37 °C in the CO_2 incubator, then the absorbance of formazan was measured using Elisa Plate Reader at 490 nm, and then converted to cell number using a calibration curve.

In order to study cell morphology and cell distribution on the vascular constructs, the cells were stained with FITC-conjugated phalloidin and DAPI for actin filaments and nuclei, respectively. After culture, the cells within the constructs were fixed with 4% PFA for 30 min at RT. The cells were permeabilized in 0.1% Triton X-100 solution for 5 min at RT and washed with PBS. The samples were incubated in the blocking solution of 1% BSA (w/v) for 30 min at 37 °C, and then incubated in FITC-phalloidin (1:100, Sigma, USA) for 1 h at 37 °C. After washing with PBS, the samples were counterstained with DAPI (1:5000, in PBS) for 10 min at RT and examined with a laser scanning confocal microscope (LSCM, Zeiss LSM700)

The expressions of endothelial cell markers, CD31 and vWF, of HUVECs lining the lumen of the vascular construct were investigated by immunocytochemistry. 1.5×10^5 cells were seeded onto the lumen side of each vascular construct, and then incubated at 37 °C in a humidified 5% CO_2 incubator for three days. At the end of the three day culture, the cells were fixed with 4% PFA for 2 h at RT. The samples were introduced to 100 mM glycine for 10 min, washed with PBS three times, permeabilized with 0.1% Triton X-100 (in PBS) for 10 min at RT, and washed with PBS again. The samples were incubated in a blocking solution of 1% BSA (in PBS) for 30 min at 37 °C. The cells were incubated with primary antibody against vWF overnight at + 4 °C, and then secondary antibody goat anti-rabbit Alexa Fluor 488 was applied for 1 h at 37 °C. Afterward, the cells were incubated with primary antibody against CD31 overnight at + 4 °C, and then treated with secondary antibody (goat anti-mouse Alexa Fluor 555) for 1 h at 37 °C. The cells were counterstained with DAPI (1:5000) for 10 min at RT and examined with LSCM.

The endothelial cell morphology on the vascular construct was examined with SEM. After freeze-drying the vascular constructs containing endothelial cells, the samples were coated with gold under vacuum by a sputter coater (Quorum, Q15RS) and then examined with SEM (Zeiss, Evo10).

Acknowledgements

This study was supported by the Scientific and Technological Research Council of Turkey (TUBITAK) SBAG 118S587 and TUBITAK-BIDEB 2210-C program, and these grants were gratefully acknowledged.

Conflict of Interest

The authors declare no conflict of interest.

Data Availability Statement

The data that support the findings of this study are available from the corresponding author upon reasonable request.

Keywords

biomimetic, circumferentially aligned electrospun fibers, endothelization, polyesters, tri-layered vascular constructs

Received: August 11, 2023
Revised: December 18, 2023
Published online: December 28, 2023

[1] World Health Organization Cardiovascular diseases (CVDs), https://www.who.int/news-room/fact-sheets/detail/cardiovascular-diseases-(cvds), (accessed 07, **2023**).

[2] C. W. Tsao, A. W. Aday, Z. I. Almarzooq, C. A. M. Anderson, P. Arora, C. L. Avery, C. M. Baker-Smith, A. Z. Beaton, A. K. Boehme, A. E. Buxton, Y. Commodore-Mensah, M. S. V. Elkind, K. R. Evenson, C. Eze-Nliam, S. Fugar, G. Generoso, D. G. Heard, S. Hiremath, J. E. Ho, R. Kalani, D. S. Kazi, D. Ko, D. A. Levine, J. Liu, J. Ma, J. W. Magnani, E. D. Michos, M. E. Mussolino, S. D. Navaneethan, N. I. Parikh, et al., *Circulation* **2023**, *147*, 93.
[3] S. C. Schutte, R. M. Nerem, in: *Biomater. Sci.* (Eds.: B.D. Ratner, A.S Hoffman, F.J. Schoen, J.E. Lemons), Academic Press, Cambridge **2013**, *3*, Ch. II.6.9.
[4] S. Pashneh-Tala, S. MacNeil, F. Claeyssens, *Tissue Eng Part B Rev* **2016**, *22*, 68.
[5] J. F. Sabik, *Circulation* **2011**, *124*, 273.
[6] D. G. Seifu, A. Purnama, K. Mequanint, D. Mantovani, *Nat Rev Cardiol* **2013**, *10*, 410.
[7] W. M. Abbott, A. Callow, W. Moore, R. Rutherford, F. Veith, S. Weinberg, *J Vasc Surg Venous Lymphat Disord* **1993**, *17*, 746.
[8] D. Miranda-Nieves, A. Ashour, E. Chaikof, in *Biomater., Artif. Organs Tissue Eng.*, (Eds.: D. Eberli, S. Lee, A. Traweger), Springer, Cham **2021**, Ch. 1.
[9] U. S. National Institutes of Health, National Cancer Institute, https://training.seer.cancer.gov/anatomy/cardiovascular/blood/physiology.html (accessed 07, **2023**).
[10] V. Hasirci, N. Hasirci, *Fundamentals of Biomaterials*, Springer, Cham **2018**. Ch. 16.
[11] M. H. Ross, W. Pawlina, *Histology: A Text and Atlas: with Correlated Cell and Molecular Biology*, Lippincott Williams & Wilkins, Philadelphia**2011**.
[12] A. G. Tabriz, C. G. Mills, J. J. Mullins, J. A. Davies, W. Shu, *Frontiers in Bioengineering and Biotechnology* **2017**, *5*, 13.
[13] Z. Xu Z, J. Li, H. Zhou, X. Jiang, C. Yang, F. Wang, P. Yuanyuan, L. Nana, L. Xiaoyan, S. Lina, S. Xiaomei, *RSC Adv.* **2016**, *6*, 43626.
[14] Y. Zhang, L. Ye, **2011**, *50*, 776.
[15] D. Yucel, G. T. Kose, V. Hasirci, *Biomaterials* **2010**, *31*, 1596.
[16] Z. Niu, X. Wang, X. Meng, X. Guo, Y. Jiang, Y. Xu, Q. Li, C. Shen, *Biomed. Mater.* **2019**,*14*, 035006.
[17] B. P. Chan, K. W. Leong, *Eur Spine J* **2008**, *17*, 467.
[18] K. Iwasaki, K. Kojima, S. Kodama, A. C. Paz, M. Chambers, M. Umezu, C. A. Vacanti, *Circulation* **2008**, *118*, 52.
[19] S. I. Jeong, S. Y. Kim, S. K. Cho, M. S. Chong, K. S. Kim, H. Kim, S. B. Lee, Y. M. Lee, *Biomaterials* **2007**, *28*, 1115.
[20] S. Koch, T. C. Flanagan, J. S. Sachweh, F. Tanios, H. Schnoering, T. Deichmann, V. Ellä, M. Kellomäki, N. Gronloh, T. Gries, R. Tolba, T. Schmitz-Rode, S. Jockenhoevel, *Biomaterials* **2010**, *31*, 4731.
[21] J. Zhao, H. Qiu, D. L. Chen, W. X. Zhang, D. C. Zhang, M. Li, *Int. J. Biol. Macromol.* **2013**, *56*, 106.
[22] C. B. Weinberg, E. Bell, *Science* **1986**, *231*, 397.
[23] L. E. Niklason, J. Gao, W. M. Abbott, K. K. Hirschi, S. Houser, R. Marini, R. Langer, *Science* **1999**, *284*, 489.
[24] D. Schmidt, S. P. Hoerstrup, *Swiss Med Wkly* **2006**, *136*, 618.
[25] S. G. Wise, M. J. Byrom, A. Waterhouse, P. G. Bannon, A. S. Weiss, M. K. Ng, *Acta Biomater.* **2011**, *7*, 295.
[26] P. Zorlutuna, P. Vadgama, V. Hasirci, *J Tissue Eng Regen Med* **2010**, *4*, 628.
[27] H. Wu, J. Fan, C. C. Chu, J. Wu, *J Mater Sci Mater Med* **2010**, *21*, 3207.
[28] X. Zhang, V. Thomas, Y. Xu, S. L. Bellis, Y. K. Vohra, *Biomaterials* **2010**, *31*, 4376.
[29] M. X. Li, L. Li, S. Y. Zhou, J. H. Cao, W. H. Liang, Y. Tian, X. T. Shi, X. B. Yang, D. Y. Wu, *RSC Adv.* **2021**, *11*, 31783.
[30] W. Jia, M. Li, H. Weng, G. Gu, Z. Chen, *Mater Sci Eng C Mater Biol Appl* **2020**, *110*, 110717.
[31] T. Wu, J. Zhang, Y. Wang, D. Li, B. Sun, H. El-Hamshary, M. Yin, X. Mo, *Mater Sci Eng C Mater Biol Appl* **2018**, *82*, 121.
[32] X. Yuan, W. Li, B. Yao, Z. Li, D. Kong, S. Huang, M. Zhu, *Polymers* **2022**, *14*, 1370.
[33] R. Huang, X. Gao, J. Wang, H. Chen, C. Tong, Y. Tan, Z. Ta, *Ann Biomed Eng* **2018**, *46*, 1254.
[34] K. Liu, N. Wang, W. Wang, L. Shi, H. Li, F. Guo, L. Zhang, L. Kong, S. Wang, Y. Zhao, *J. Mater. Chem. B* **2017**, *5*, 3758.
[35] Y. Zhang, H. Ouyang, C. T. Lim, S. Ramakrishna, Z. M. Huang, *J. Biomed. Mater. Res., Part B* **2005**, *72*, 156.
[36] Y. Gou, C. Liu, T. Lei, F. Yang, presented at *Int. Conf. Manipulation, Manuf. Meas. Nanoscale*, Taipei, Taiwan, October, **2014**.
[37] R. Dorati, E. Chiesa, S. Pisani, I. Genta, T. Modena, G. Bruni, C. R. M. Brambilla, M. Benazzo, B. Conti, *J Drug Deliv Sci Technol* **2020**, *58*, 101781.
[38] A. J. Robinson, A. Pérez-Nava, S. C. Ali, J. B. González-Campos, J. L. Holloway, E. M. Cosgriff-Hernandez, *Matter* **2021**, *4*, 821.
[39] Q. P. Pham, U. Sharma, A. G. Mikos, *Biomacromolecules* **2006**, *7*, 2796.
[40] C. Liu, C. Zhu, J. Li, P. Zhou, M. Chen, H. Yang, B. Li, *Bone Res.* **2015**, *3*, 15012.
[41] R. Delaine-Smith, N. Green, S. Matcher, S. Macneil, G. Reilly, *PLoS One* **2014**, *9*, e89761.
[42] F. Guo, N. Wang, L. Wang, L. Hou, L. Ma, J. Liu, Y. Chen, B. Fan, Y. Zhao, *J. Mater. Chem. A* **2015**, *3*, 4782.
[43] M. Stekelenburg, M. C. Rutten, L. H. Snoeckx, F. P. Baaijens, *Tissue Eng Part A* **2009**, *15*, 1081.
[44] M. J. McClure, S. A. Sell, D. G. Simpson, B. H. Walpoth, G. L. Bowlin, *Acta Biomater.* **2010**, *6*, 2422.
[45] M. A. Fahad, M. S. Rahaman, M. S. I. Mahbub, M. Park, H.-Y. Lee, B.-T. Lee, *Mater. Des.* **2022**, *225*, 111488.
[46] M. T. H. K. A. McKenna, R. C. Sarao, P. C. Wu, C. L. Maslen, R. W. Glanville, D. Babcock, K. W. Gregory, *Acta Biomater.* **2012**, *8*, 225.
[47] K. Y. Law, *J. Phys. Chem. Lett.* **2014**, *5*, 686.
[48] X. Wang, P. Lin, Q. Yao, C. Chen, *World J. Surg.* **2007**, *31*, 682.
[49] J. Wu, C. Hu, Z. Tang, Q. Yu, X. Liu, H. Chen, *Colloid Interface Sci. Commun.* **2018**, *23*, 34.
[50] L. Soletti, Y. Hong, J. Guan, J. J. Stankus, M. S. El-Kurdi, W. R. Wagner, D. A. Vorp, *Acta Biomater.* **2010**, *6*, 110.
[51] M. Ahmed, H. Ghanbari, B. G. Cousins, G. Hamilton, A. M. Seifalian, *Acta Biomater.* **2011**, *7*, 3857.